CHAPTER 3

Result and discussion

3.1 Static calculation

3.1.1 Optimized structures and Infrared spectra

The optimized structures of 3HF and 3HF with protic solvent, 3HF with ammonia (3HF(NH_3)), 3HF with methanol (3HF(CH_3OH)) and 3HF with wa ter (3HF(H_2O)) in S_0 and S_1 states have been calculated using B3LYP and TD-B3LYP with TZVP basis set. All structures have been optimized and analysis of vibrational frequency is done to ensure the validity of the stationary point. In order to explain the mechanism of PT, the atoms associated with the hydrogen bonding were labeled using serial number and the dash line refers to the intra- and intermolecular hydrogen bond as shown in Figure 3.1.

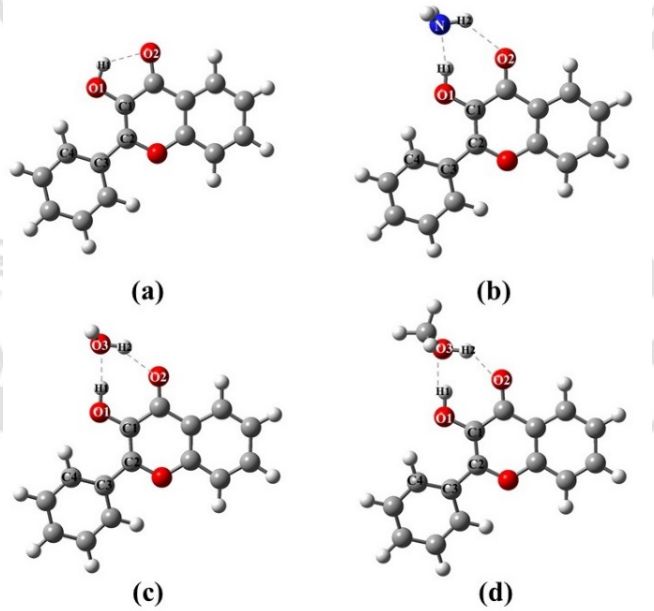

Figure 3.1 The ground state optimized structures of 3HF and its complexes: (a) 3HF, (b) 3HF(NH_3), (c) 3HF(CH_3OH) and (d) 3HF(H_2O) computed at B3LYP/TZVP level.

Table 3.1 The important distances (Å) of 3HF, 3HF(NH_3), 3HF(CH_3OH) and 3HF(H_2O) enol forms involving PT process in S_0 and S_1 states.

Complex	State	Distance (Å)							
		O1–H1	**S–H2**	**O2···H1**	**S···H1**	**O2···H2**	**O1···O2**	**O1···S**	**O2···S**
3HF	S_0	0.980	-	1.976	-	-	2.606	-	-
	S_1	1.011	-	1.760	-	-	2.500	-	-
3HF(NH_3)	S_0	1.003	1.016	2.370	1.764	2.181	2.771	2.757	2.903
	S_1	1.064	1.020	2.403	1.536	2.034	2.772	2.597	2.790
3HF(CH_3OH)	S_0	0.991	0.975	2.382	1.730	1.838	2.789	2.720	2.700
	S_1	1.031	0.988	2.410	1.526	1.710	2.800	2.557	2.600
3HF(H_2O)	S_0	0.987	0.977	2.378	1.762	1.828	2.789	2.749	2.700
	S_1	1.020	0.989	2.402	1.575	1.709	2.798	2.593	2.603

S represents the heavy atoms of solvent molecules (O3 and N in Figure 3.1)

The optimized structures of 3HF and 3HF with protic solvent, 3HF with ammonia ($3HF(NH_3)$), 3HF with methanol ($3HF(CH_3OH)$) and 3HF with water ($3HF(H_2O)$) in S_0 and S_1 states have been calculated using B3LYP and TD-B3LYP with TZVP basis set. All structures have been optimized and analysis of vibrational frequency is done to ensure the validity of the stationary point. In order to explain the mechanism of PT, the atoms associated with the hydrogen bonding were labeled using serial number and the dash line refers to the intra- and intermolecular hydrogen bond as shown in Figure 3.1.

The important distances of enol forms of 3HF and its complexes involved in PT process are listed in Table 3.1. For 3HF, bond distance of O1–H1, O2···H1 and O1···O2 are 0.980, 1.976 and 2.606 Å, respectively in S_0 state. Upon photoexcitation, the O1–H1 bond is lengthened to 1.011 Å whereas distance of O2···H1 and O1···O2 are shortened to 1.760 and 2.500 Å in S_1 state. The changes of distances (O1–H1, O2···H1 and O1···O2) indicate that intramolecular hydrogen bonds are strengthened in S_1 state.

For $3HF(NH_3)$, the bond lengths of O1–H1 and S–H2 change from S_0 state 1.003 and 1.016 Å to S_1 state 1.064 and 1.020 Å. The distances of S···H1 and O2···H2 are 1.764 and 2.181 Å in S_0 state while these distances are decreased to 1.536 and 2.034 Å, respectively in S_1 state. The distances of O1···S and O2···S are decreased from 2.757 Å and 2.903 Å in S_0 state to 2.597 Å and 2.790 Å in S_1 state. In addition, the bond length of O1–H1, O2···H1, and O1···O2 are lengthened in S_1 state while intermolecular hydrogen bonds (S···H1 and O2···H2) and distance of heavy atom (O1···O2, O1···S and O2···S) are also shortened. Similarly, for $3HF(CH_3OH)$, the calculated bond length of O1–H1 and S–H2 are 0.991 and 0.975 Å in S_0 state, whereas, the corresponding bond lengths in the S_1 state are elongated to 1.031 Å and 0.988 Å, respectively. It is interesting that the bond distance of intermolecular hydrogen bonds (S···H1 and O2···H2) are 1.730 and 1.838 Å in S_0 state while these distances are shortened to 1.526 and 1.710 Å, respectively in S_1 state. The distance of O1···S and O2···S, which are heavy atom between 3HF and methanol, are decreased from 2.720 Å and 2.700 Å in S_0 state to 2.557 Å and 2.600 Å in S_1 state. For $3HF(H_2O)$, it can be found that O1–H1 and S–H2 are 0.987 and 0.977 Å in S_0 state, however, these bonds change to be 1.020 and 0.989 Å. The bond distance of S···H1 and O2···H2 are 1.762 and 1.828 Å in S_0 state while these distances are shortened to 1.575 and 1.709 Å, respectively in S_1 state. The distance of O1···S and O2···S are

decreased from 2.749 Å and 2.700 Å in S_0 state to 2.593 Å and 2.603 Å in S_1 state. Hence, such changes in bond distances indicate that the intermolecular hydrogen bonds **(**S···H1 and O2···H2**)** are all strengthened for 3HF(NH_3), 3HF(CH_3OH) and 3HF(H_2O) in S_1 state.

Furthermore, considering the spectral shift (red-shift or blue-shift) of some characteristic vibration mode can be predict strengthening or weakening of S_1 state hydrogen bond as proposed by Zhao and Han [55]. Therefore, investigating the vibrational frequencies of O1–H1 and S–H2 stretching involved in hydrogen bonding should provide a clear-cut signature of hydrogen bonding dynamics. The infrared (IR) spectra are calculated by B3LYP and TD-B3LYP with TZVP basis set. Analysis vibrational frequencies of the O–H stretching mode of 3HF is shown in Figure 3.2 and 3HF with protic solvents are depicted in Figure 3.3 and listed in Table 3.2. From the results, there is only one mode of O–H stretching mode for 3HF molecule as shown in Figure 3.2. The blue color represents O–H stretching vibrational frequencies for 3HF which is located at 3540, whereas it changes to 3047 cm^{-1} in S_1 state. The red-shift is 493 cm^{-1} indicates that the intramolecular hydrogen bond is strengthened in S_1 state.

Table 3.2 The vibrational frequencies of the O–H and N–H stretching vibrations involving PT process of 3HF, 3HF(NH_3), 3HF(CH_3OH) and 3HF(H_2O) in the S_0 and S_1 states.

Bond	State	Wavenumber (cm^{-1})			
		3HF	**3HF(NH_3)**	**3HF(CH_3OH)**	**3HF(H_2O)**
O1–H1	S_0	3540	3063	3277	3349
	S_1	3047	2118	2588	2800
$\Delta\tilde{\nu}$		493	945	689	549
S–H2	S_0	-	3585	3597	3576
	S_1	-	3428	3375	3364
$\Delta\tilde{\nu}$		-	157	222	212

S represents the heavy atoms of solvent molecules **(**O3 and N in Figure 3.1**)**

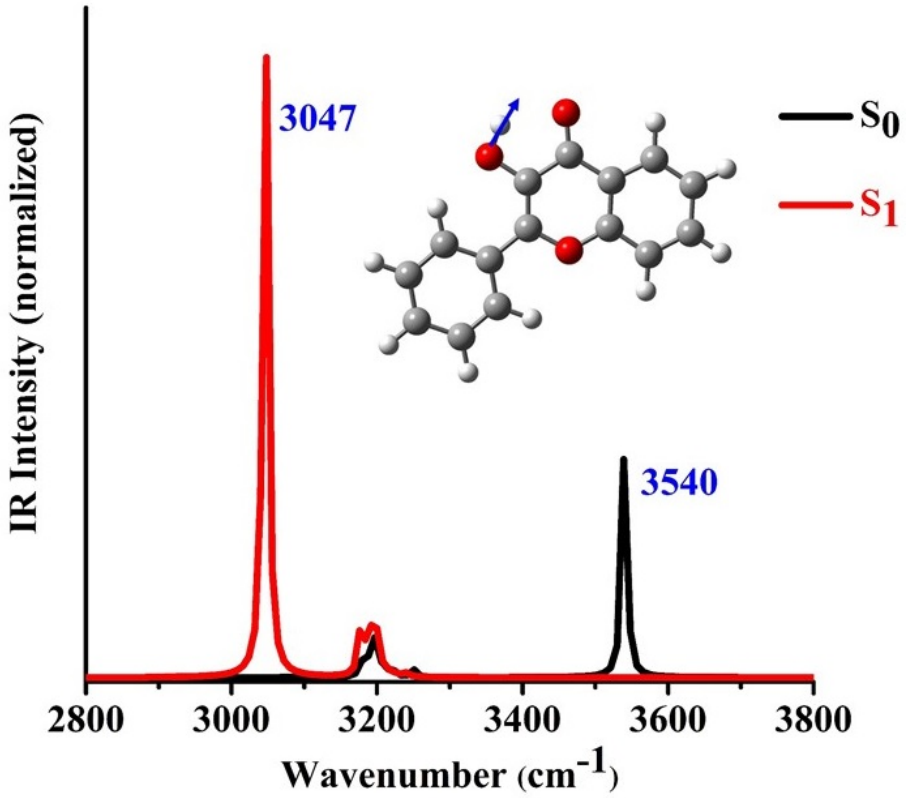

Figure 3.2 Simulated IR spectra in S_0 and S_1 of 3HF at the spectral region of O1–H1 (blue) stretching band computed at B3LYP and TD-B3LYP with TZVP basis set.

For 3HF(NH_3), exhibiting one mode of O–H stretching from 3HF molecule (blue) and one mode of N–H stretching from ammonia (pink), the O–H stretching in S_0 state is located at 3063 cm^{-1} and 2118 cm^{-1} in S_1 state. The N–H stretching appears in region of 3585 cm^{-1} in S_0 state and 3428 cm^{-1} after excitation. For 3HF(CH_3OH) and 3HF(H_2O), vibrational frequencies of O–H stretching are exhibited two mode, which are first mode from 3HF molecule (blue) and second mode from solvent (pink), first mode of O–H stretching mode appear in region of 3277 and 3349 cm^{-1} in S_0 state, while it changes to be 2588 and 2800 cm^{-1} in S_1 state, respectively and second mode of O–H stretching are changed from 3597 and 3576 cm^{-1} in S_0 to 3375 and 3364 cm^{-1} in S_1 state, respectively.

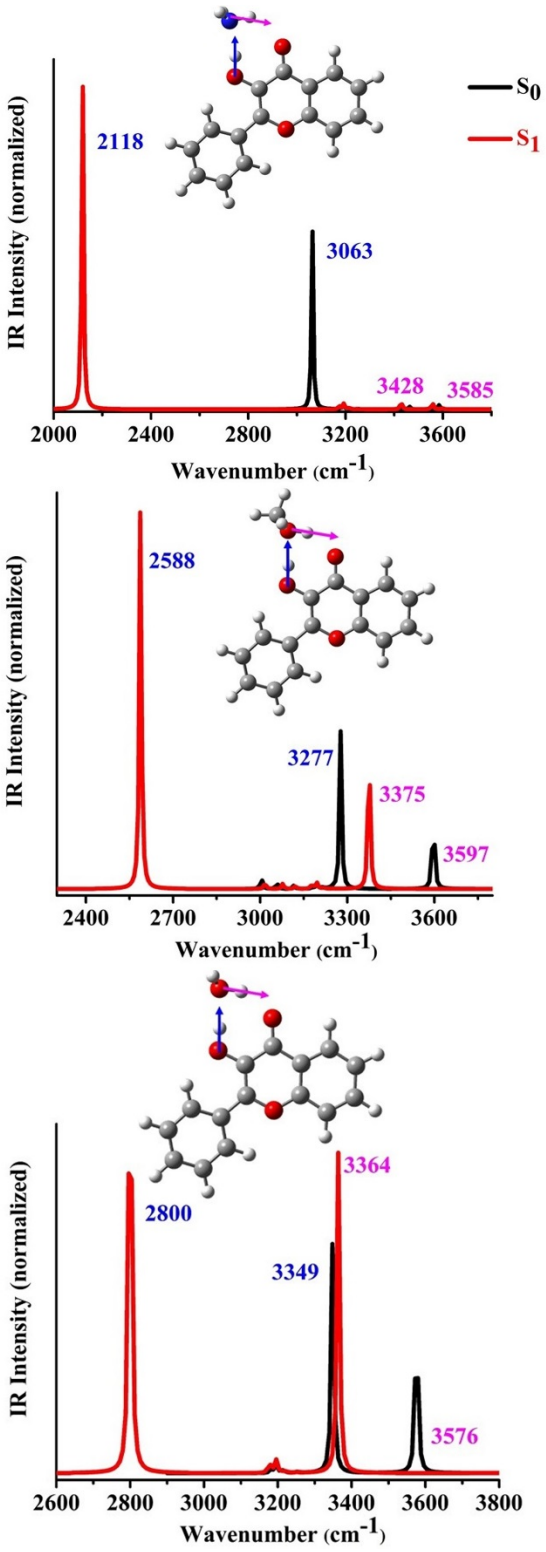

Figure 3.3 Simulated IR spectra in S_0 and S_1 of (a) 3HF(NH_3), (b) 3HF(CH_3OH) and (c) 3HF(H_2O) at the spectral region of O1–H1 (blue) and N–H2 or O3–H2 (pink) stretching bands computed at B3LYP and TD-B3LYP with TZVP basis set.

From the results, it can be found that the first vibrational frequencies of O1–H1 stretching mode of 3HF(NH_3), 3HF(CH_3OH) and 3HF(H_2O) are red-shift around 945, 689 and 549 cm^{-1}, respectively and the second vibrational frequencies of S–H2 stretching mode are red-shift 1572, 22 and 212 cm^{-1}. These large red-shifts illustrate that intermolecular hydrogen bond become strengthen in S_1 state, therefore, it can be assumed that the first proton may be transferred from 3HF molecule (O1–H1---S) to the solvent after that the second proton is transferred from solvent molecule to proton accepter of 3HF because of the large red-shift.

3.1.2 Electronic spectra and frontier molecular orbitals (MOs)

The absorption and emission spectra of 3HF and its complexes have been simulated by using TD-B3LYP/TZVP level, which are based on their optimized S_0 and S_1 structures, respectively. Simulated absorption and emission spectra of all complexes are plotted in Figure 3.4. The maximum wavelengths, electronic transition energies, MOs contributions and oscillator strengths (*f*) of all complexes are summarized in Table 3.

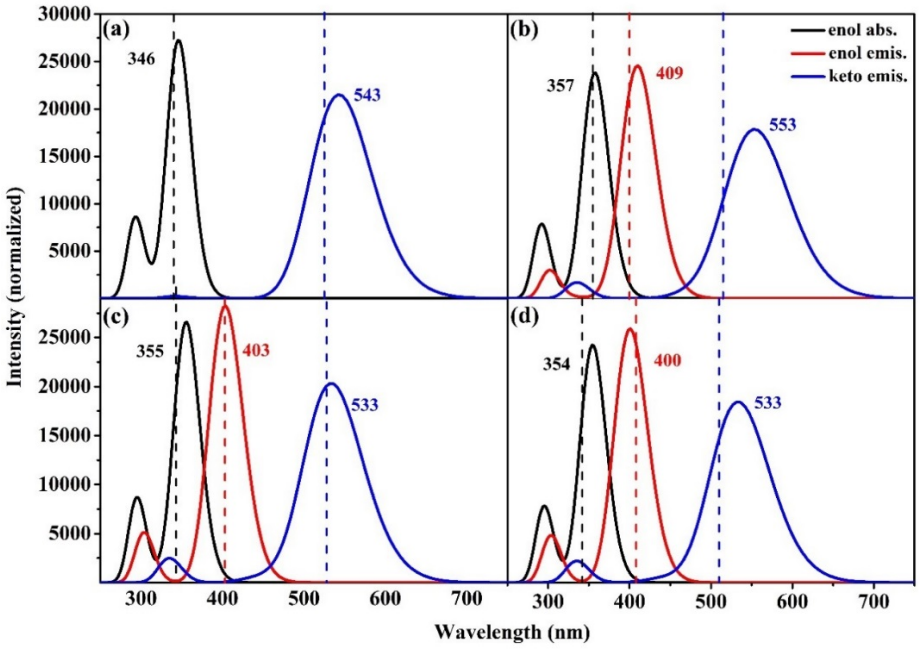

Figure 3.4 Simulated absorption and emission spectra of a) 3HF, (b) 3HF(NH_3), (c) 3HF(CH_3OH) and (d) 3HF(H_2O) computed at TD-B3LYP/TZVP level. The maximum wavelengths of absorption and emission spectra from the experimental data are shown in dashed lines [30, 56].

Table 3.3 Electronic and photophysical properties of 3HF and its complexes computed at TD-B3LYP/TZVP level in gas phase. Calculated the maximum wavelengths (λ_{max}) of absorption and emission (nm), oscillator strength (*f*), excitation energy (eV) and molecular orbitals (MOs).

Complex	Absorption				Emission				Stokes shift
	Enol form				Enol form		Keto form		
	nm	*f*	eV	MOs contributions	nm	*f*	nm	*f*	
3HF	346	0.376	3.58	HOMO →LUMO (97%)	-	-	543	0.338	197
3HF(NH_3)	357	0.351	3.47	HOMO →LUMO (97%)	409	0.362	553	0.434	196
3HF(CH_3OH)	355	0.367	3.49	HOMO →LUMO (97%)	403	0.390	533	0.406	178
3HF(H_2O)	354	0.369	3.50	HOMO →LUMO (97%)	400	0.395	533	0.355	179

As shown in Figure 3.4a, the theoretical results of 3HF show that, the absorption peak is located at 346 nm with oscillator strengthh (*f*) of 0.376 while the emission peak is observed at 543 nm with oscillator strength (*f*) of 0.338, which is close to the experimental value of 340 (absorption peak) and 525 nm (emission peak) [30] (dashed line in Figure 3.4). A deviation of 197 nm between absorption and emission peak is described as large Stokes shift. For 3HF with protic solvents, it has been found that the absorption peaks of 3HF(NH_3), 3HF(CH_3OH) and 3HF(H_2O) are located at 357, 355 and 354 nm, respectively, which are coincidence that the absorption peak are about 355, 343 and 342 nm, respectively, in experiment. For 3HF(NH_3), the simulated results indicate an emission peak at 409 and 553 nm, which are also in agreement with experimental result due to the experiment reported fluorescence peak, that of enol and keto form at 400 and 515 nm, respectively. The emission peak of enol and keto form construction of 3HF(CH_3OH) at 403 and 533 nm is greatly close to experimental value of 403 and 528 nm, respectively. For 3HF(H_2O), the emission peak of enol form and keto form are observed at 400 and 533 nm, which are also consistent with experimental result of 408 and 510 nm, respectively. In addition, it should be remarked that the large Stokes shift values are 196, 178 and 179 nm.

Next, to describe the nature of the S_1 state, the charge distribution in the electronic excited state should be investigated. The frontier MOs of the 3HF and its complexes are shown in Figure 3.5. Herein, only the highest occupied molecular orbital (HOMO) and the lowest unoccupied molecular orbital (LUMO) are shown for all complexes because electronic transition is mainly associated with these orbitals in rage of 97% (HOMO → LUMO). The π character of HOMO and π* character of LUMO can be seen clearly, which is corresponded to π to π* transition. It should be noted that the HOMO and LUMO are localized on different parts of the molecules. From the HOMO orbitals, the electron density is localized on the phenyl moiety and partially on the pyranyl ring. While in the LUMO orbitals, it is can be seen that the electron density completely occupies the whole molecule. Upon photoexcitation, the electron density of the carbonyl (C=O) group increases (become more basic) and that of the hydroxy (–OH) group decreases (become more acid), giving the driving force to the PT process involved in the intramolecular hydrogen bond (O–H···O). Therefore, the ESPT process could occur because of intramolecular charge transfer.

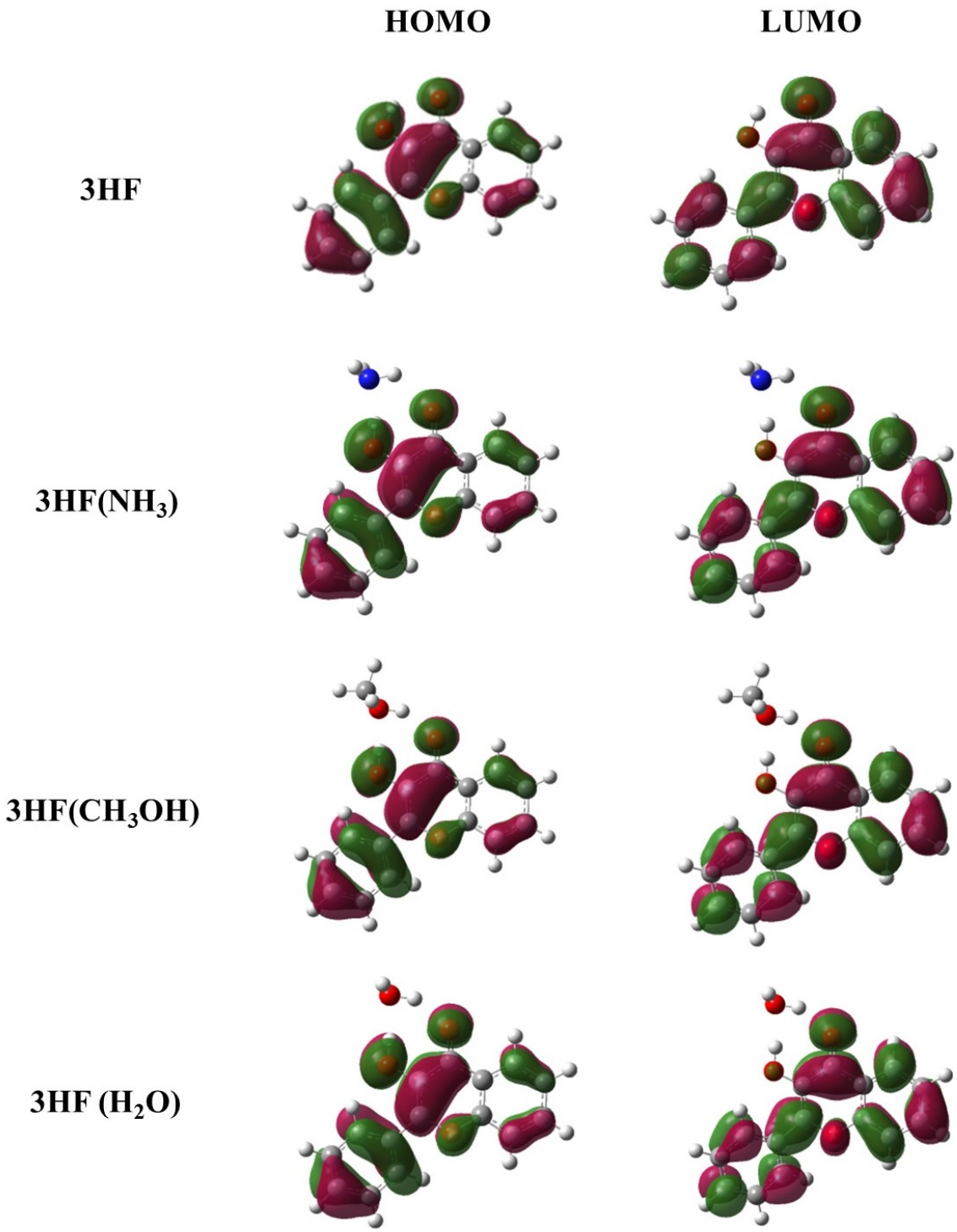

Figure 3.5 The frontier molecular orbitals of enol forms of 3HF, 3HF(NH_3), 3HF(CH_3OH) and (d) 3HF(H_2O).

3.1.3 Potential energy curves of ESPT reactions

To understand the detailed mechanism of ESPT clearly, PECs involving PT coordinates of 3HF and its complexes both in the S_0 and S_1 states are scanned by using B3LYP and TD-B3LYP method, respectively. B3LYP has been proven to be reliable to provide the shape of PECs of PT reaction compared with higher levels [57]. The constructed PECs of S_0 and S_1 states as functions of O1–H1 bond length in step of 0.05 Å (see in Figure 3.6-3.9). For 3HF, Figure 3.6 demonstrates transferring the proton H1 to O2 through intramolecular hydrogen bond with a high PT barrier of around 13.68 kcal/mol in S_0 state and a low PT barrier of 1.99 kcal/mol in S_1 state which are consistent with PT barriers reported by previous work [40, 58]. For 3HF with protic solvents, all complexes 3HF(NH_3), 3HF(CH_3OH) and 3HF(H_2O) display transferring the proton through intermolecular hydrogen bond, high PT barriers of 16.17, 18.20 and 20.16 kcal/mol are found in S_0 state while corresponding low barriers of 3.81, 3.62 and 5.64 kcal/mol, respectively are observed in S_1 state. It can be concluded that PT process occurs in S_0 state may be difficult, however the PT process is likely to proceed in S_1 state. Comparison of PT barrier of all systems suggests that PT reaction in the S_1 state should easily occur through the intramolecular hydrogen-bond that the intermolecular hydrogen-bonded next work of protic solvents.

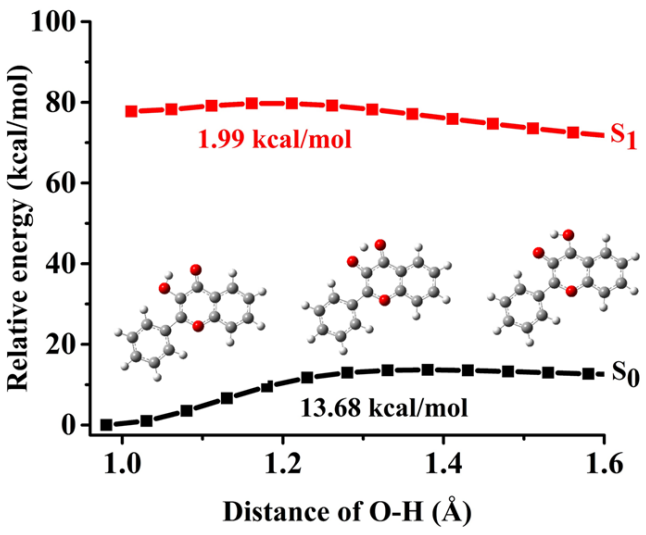

Figure 3.6 A constructed potential energy curves (PECs) in both S_0 and S_1 states as function of the O1–H1 length for 3HF.

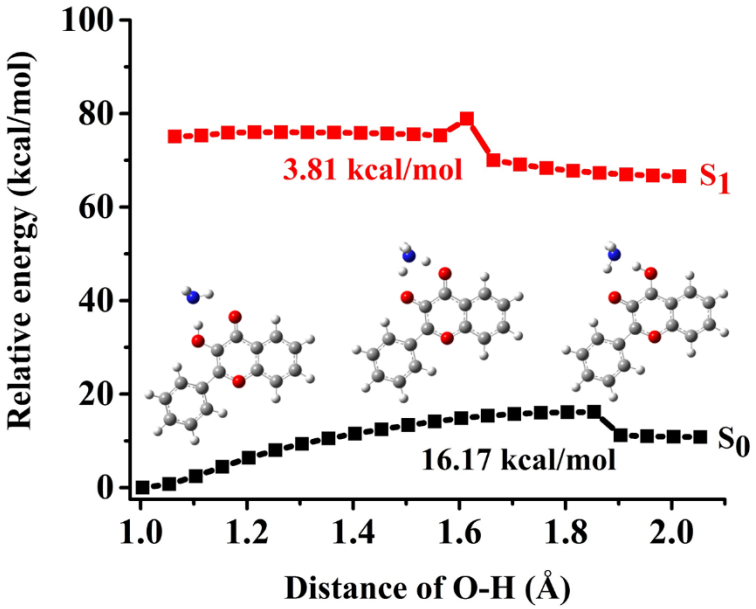

Figure 3.7 A constructed potential energy curves (PECs) in both S_0 and S_1 states as function of the O1–H1 length for 3HF(NH_3).

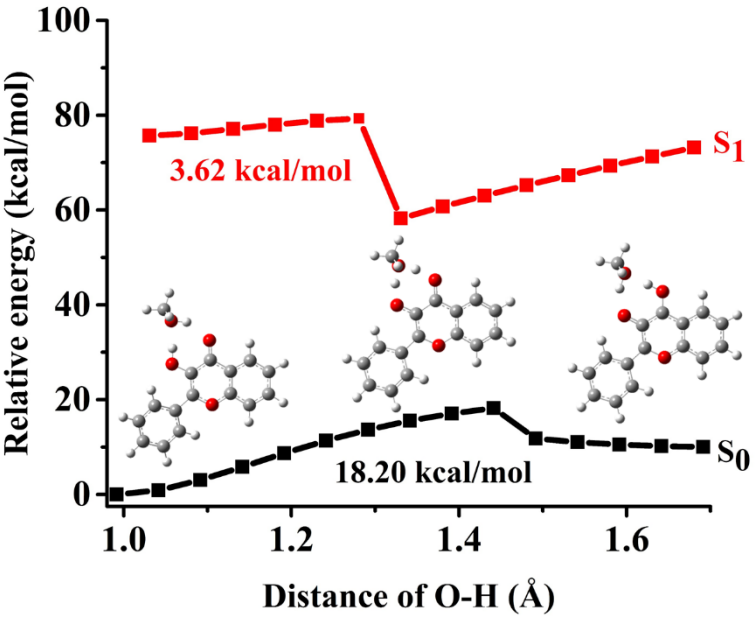

Figure 3.8 A constructed potential energy curves (PECs) in both S_0 and S_1 states as function of the O1–H1 length for 3HF(CH_3OH).

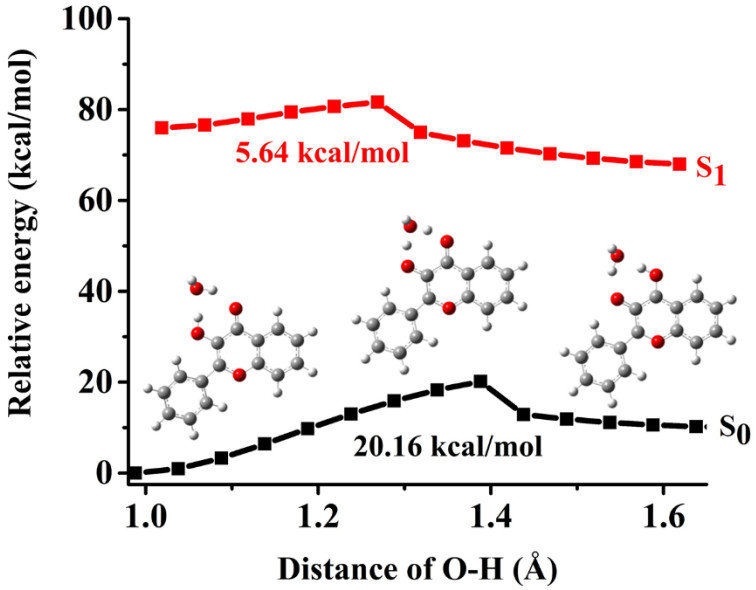

Figure 3.9 A constructed potential energy curves (PECs) in both S_0 and S_1 states as function of the O1–H1 length for 3HF(H_2O).

3.2 Dynamics simulations

Twenty-five trajectories with different initial conditions of each system were simulated to reveal the entire PT mechanisms, including pre- and post-transfer processes. All active trajectories of 3HF and 3HF with protic solvent complexes were analyzed and the statistical results are summarized in Table 3.4, which includes a number of trajectories of each type, PT probabilities, PT time, and PT barriers. The PT time is defined as the bond breaking and the bond forming distances average overall trajectories show intersects with each other, which has been used in our previous studies [59, 60]. The PT mechanisms for 3HF with protic solvents can be determined as concerted or stepwise depending on the time lag between two consecutive PTs [61]. If the time lag is shorter than about 10-15 fs, which corresponds to a vibrational period of O–H and N–H stretching modes, the PT is concerted; otherwise it is stepwise (two distinct kinetic steps via a stable intermediate).

Table 3.4 Summary of exited-state dynamics analysis of 3HF and its complexes with solvent.

Complex	ESIntraPT	ESInterPT	No PT	PT time (fs)			Probability	PT barrier (kcal/mol)
				ESIntraPT	ESIntraPT	ESInterPT		
					PT1	PT2		
3HF	20	-	5	76	-	-	0.80	1.99
3HF(NH_3)	-	9	16	-	128	259	0.36	3.81
3HF(CH_3OH)	-	10	15	-	105	117	0.40	3.62
3HF(H_2O)	-	3	22	-	100	104	0.12	5.64

3.4.1 3HF molecule

All twenty-five trajectories of 3HF show the ESIntraPT reaction within a given simulation, twenty trajectories show ESIntraPT reaction (PT probability of 80%) and five trajectories do not give PT process during simulation time. Important parameters related to PT process as a function of time are illustrated in Figure 3.11. Details of PT process can be described by a representative trajectory (Figure 3.10) using labeling atom assigned in Figure 3.1a. From Figure 3.11, the intersection between breaking (O1–H1) and forming (H1---O2) bonds indicates PT time constant at 76 fs. This PT time is in consistent with the experiment of 93 fs in *n*-octane [33]. The energy difference between excited state (S_1) and ground state (S_0) as blue line in Figure 3.11b lies above 2 eV implying that there is no skeletal change during the simulation time. The average value of torsion angle of C1C2C3C4 slightly changes around ±5 degree (Figure 3.11c), which can be seen in snapshots in Figure 3.10. More details of the PT process are depicted as follows: starting at 0 fs is enol form, then the H1 atom departs from hydroxy (proton donor) to the O2 atom of carbonyl (proton acceptor) at 76 fs after that keto is formed.

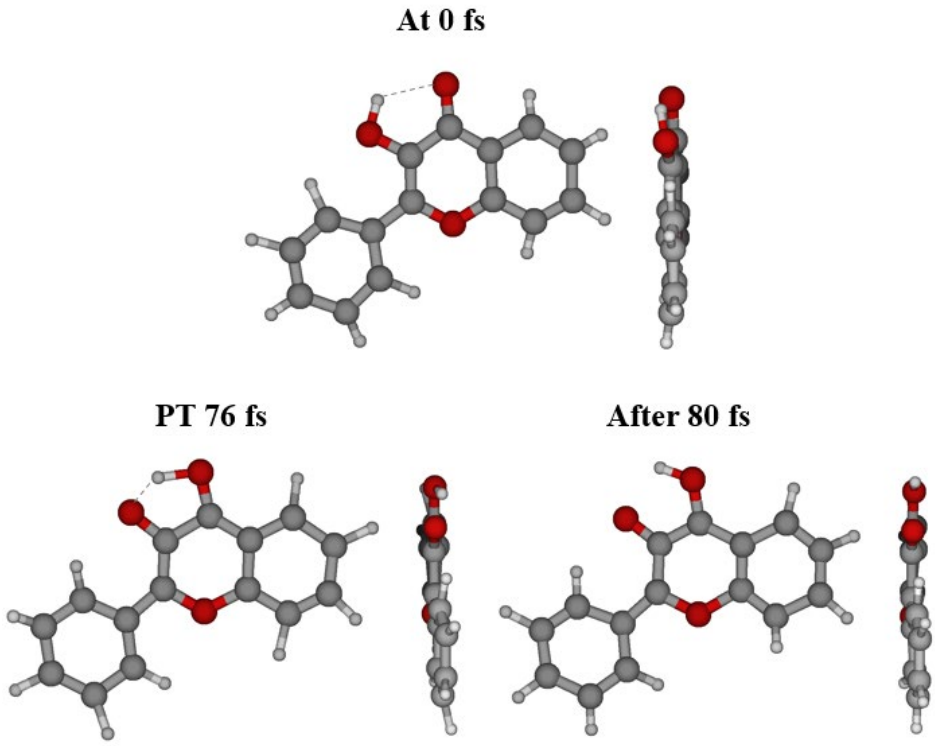

Figure 3.10 Snapshots of 3HF at different time along the ESIntraPT dynamics simulations (left: front view, right: side view).

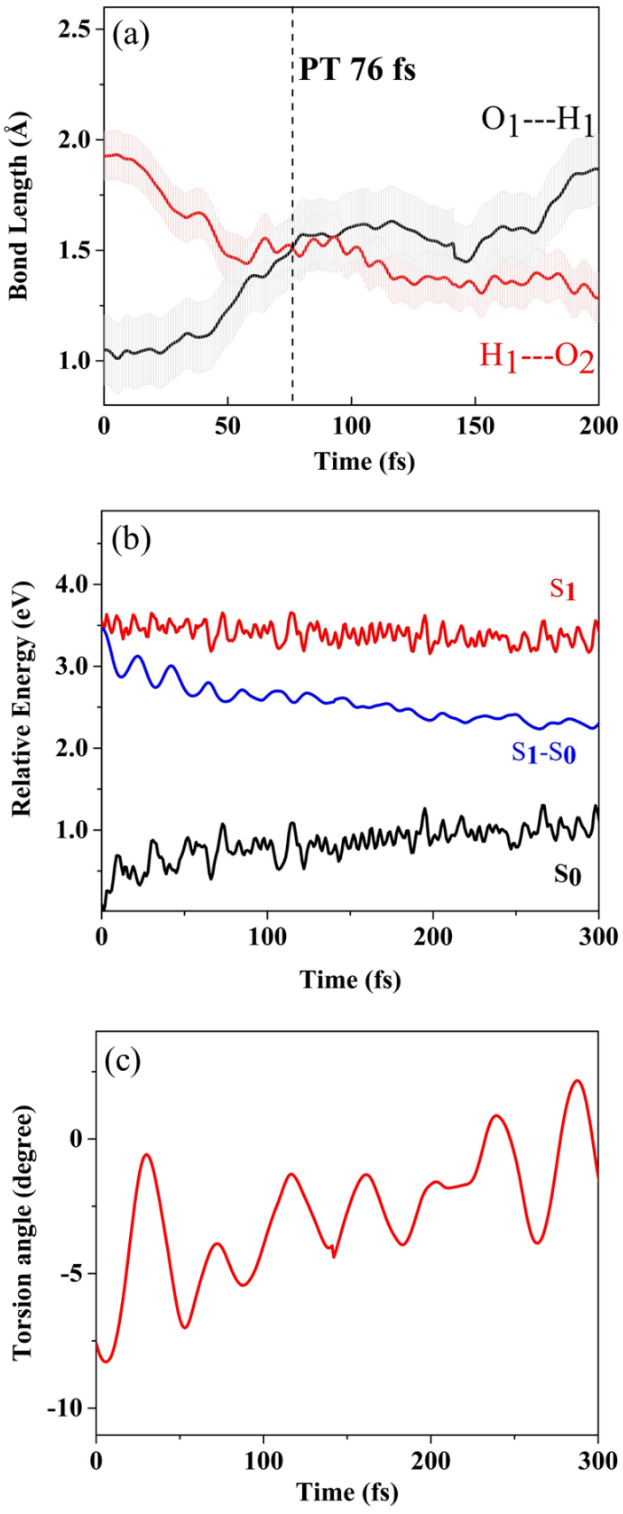

Figure 3.11 Average values over all active ESIntraPT trajectories of 3HF. (a) Time evolution of average breaking and forming bonds. The shaded areas are the standard deviation. (b) Average relative energies of excited state (S_1), ground state (S_0) and energy difference of S_1 and S_0 states (S_1- S_0). (c) Average torsion angle of 3HF.

3.4.2 3HF with one protic solvent

3.4.2.1 3HF(NH_3) complex

For 3HF(NH_3) complex, nine trajectories (36%) out of twenty-five trajectories show the ESInterPT and twenty-two trajectories do not exhibit PT reaction within a given simulation time. The important atom numbering displayed in Figure 3.1b along with time evolution of breaking and forming bonds shown in Figure 3.13a reveal that PT1 occurs at 100 fs (when the bond distances of O1---H1 and H1---N are equal) and PT2 at 104 fs (when the bond distances of O2---H2 and N---H2 are equal). The snapshots of correspond PT dynamic is displayed in Figure 3.12. The time lag of 131 fs between two PTs clearly indicates the stepwise mechanism. The different energy between two states is always above 2 eV, suggesting that there is no initial approach of conical intersection during the simulation time. The average value of torsion angle between the fused phenyl and pyranyl rings, and phenyl moiety fluctuates slightly about ±10 degree (Figure 3.13c).

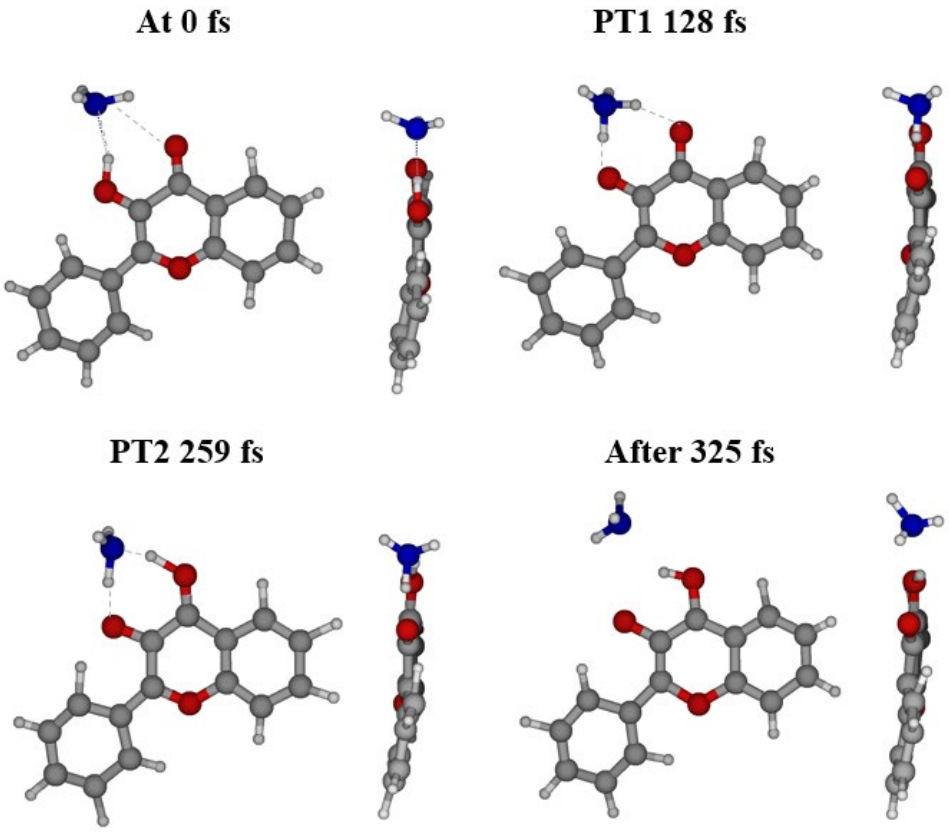

Figure 3.12 Snapshots of 3HF(NH_3) at different time along the ESInterPT dynamics simulations (left: front view, right: side view).

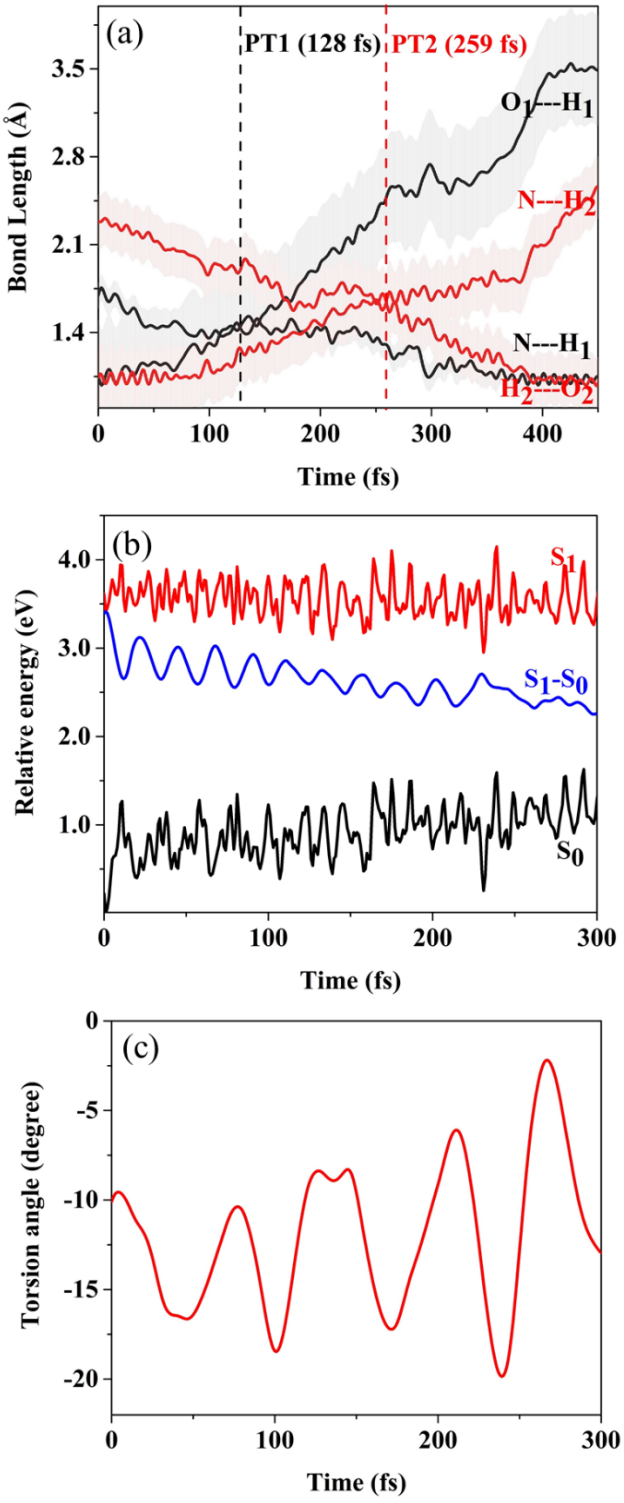

Figure 3.13 Average values over all active ESInterPT trajectories of 3HF (NH_3). (a) Time evolution of average breaking and forming bonds. The shaded areas are the standard deviation. (b) Average relative energies of excited state (S_1), ground state (S_0), and energy difference of S_1 and S_0 state (S_1-S_0). (c) Average torsion angle of 3HF(NH_3).

3.4.2.2 3HF(CH_3OH) complex

For 3HF(CH_3OH), a total of ten trajectories (40%) demonstrated ESInterPT reaction through methanol and 30 trajectories (60%) revealed no active ESInterPT within given simulation time. Using the atom numbering scheme for the intermolecular hydrogen bond from 3HF(CH_3OH) given in Figure 3.1c, the time evolutions of the two bond-forming distances (O3---H1 and O2---H2) and the two bond-breaking distances (O1---H1 and O3---H2) along the ESInterPT process average over 20 trajectories are depicted in Figure 3.15a. As the time goes, the two bond-breaking distances increase as the respective covalent bond is being broken and at the same time the two bond-forming distances decrease to covalent bond length. At 105 fs, the bond distances of O1---H1 and O3---H1 are equal (the first PT, PT1) and at 117 fs, the bond distance of O3---H2 and O2---H2 are equal (the second PT, PT2). The corresponding snapshot of these PT movements is displayed in Figure 3.14. Judging from the time lag between PT1 and PT2 (12 fs), the mechanism of ESInterPT of 3HF with methanol is concerted. The torsion angle is slightly changed during the simulation, implying that there is no initiation of internal conversion induced from skeletal change, which is supported by energy difference of S_1-S_0 lying above 2 eV.

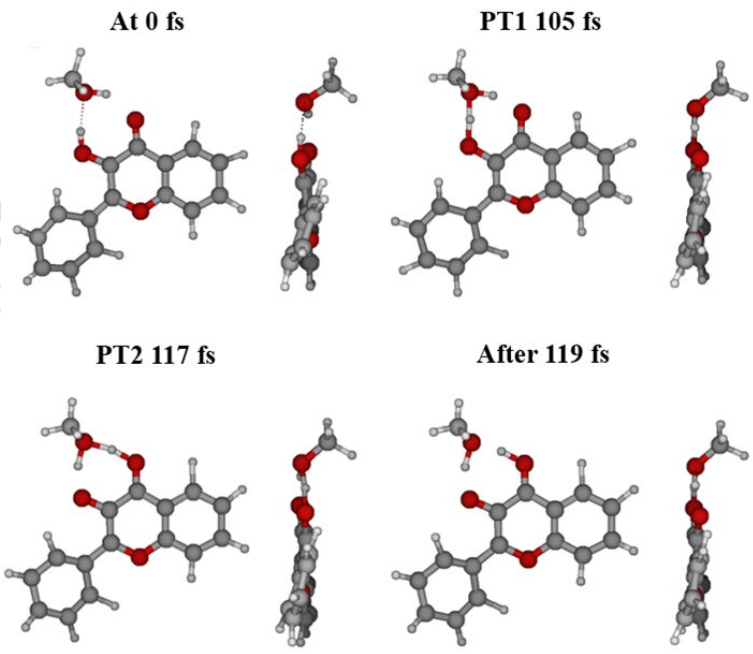

Figure 3.14 Snapshots of 3HF(**CH_3OH**) at different time along the ESInterPT dynamics simulations (left: front view, right: side view).

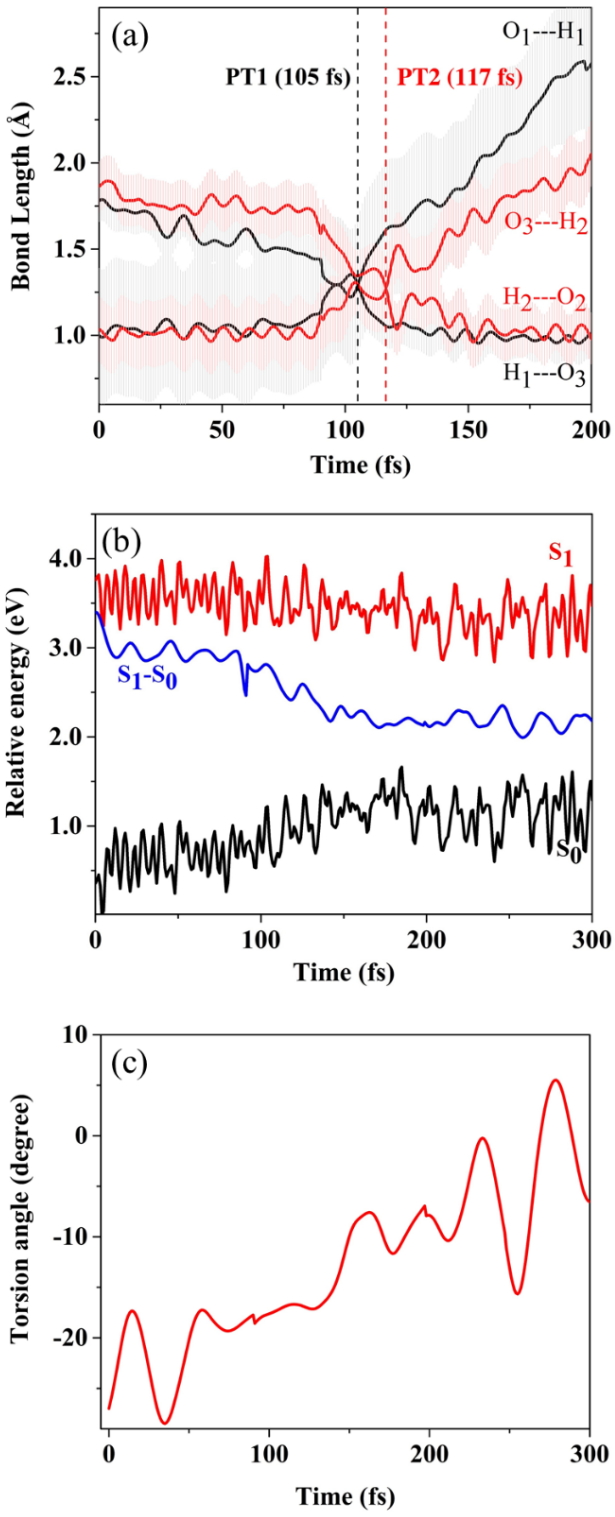

Figure 3.15 Average values over all active ESInterPT trajectories of 3HF(CH_3OH). (a) Time evolution of average breaking and forming bonds. The shaded areas are the standard deviation. (b) Average relative energies of excited state (S_1), ground state (S_0), and energy difference of S_1 and S_0 state (S_1-S_0). (c) Average torsion angle of 3HF(CH_3OH).

3.4.2.3 3HF(H_2O) complex

For 3HF(H_2O) complex, PT can occur similarly another solvent with three trajectory exhibiting ESInterPT and others without PT process. The PT probability is 12%. The atom numbering scheme for the intermolecular hydrogen bond from 3HF(H_2O) given in Figure 3.1d. The detailed PT dynamic is illustrated in Figure 3.17, in which two breaking bonds (O1---H1, O3---H2) increase and two forming bonds (O3---H1, O2---H2) decrease (see Figure 3.17a). The PT1 and PT2 are observed at 100 and 104 fs respectively. The time lag of 4 fs between PT1 and PT2 suggests that ESInterPT of 3HF(H_2O) is concerted. Snapshots of the PT dynamics simulation is depicted in Figure 3.16. Moreover, the S1-S0 (Figure 3.17b) and torsion angle (C1C2C3C4, Figure 3.17c) show that the skeleton is kept rather planar during the simulation time.

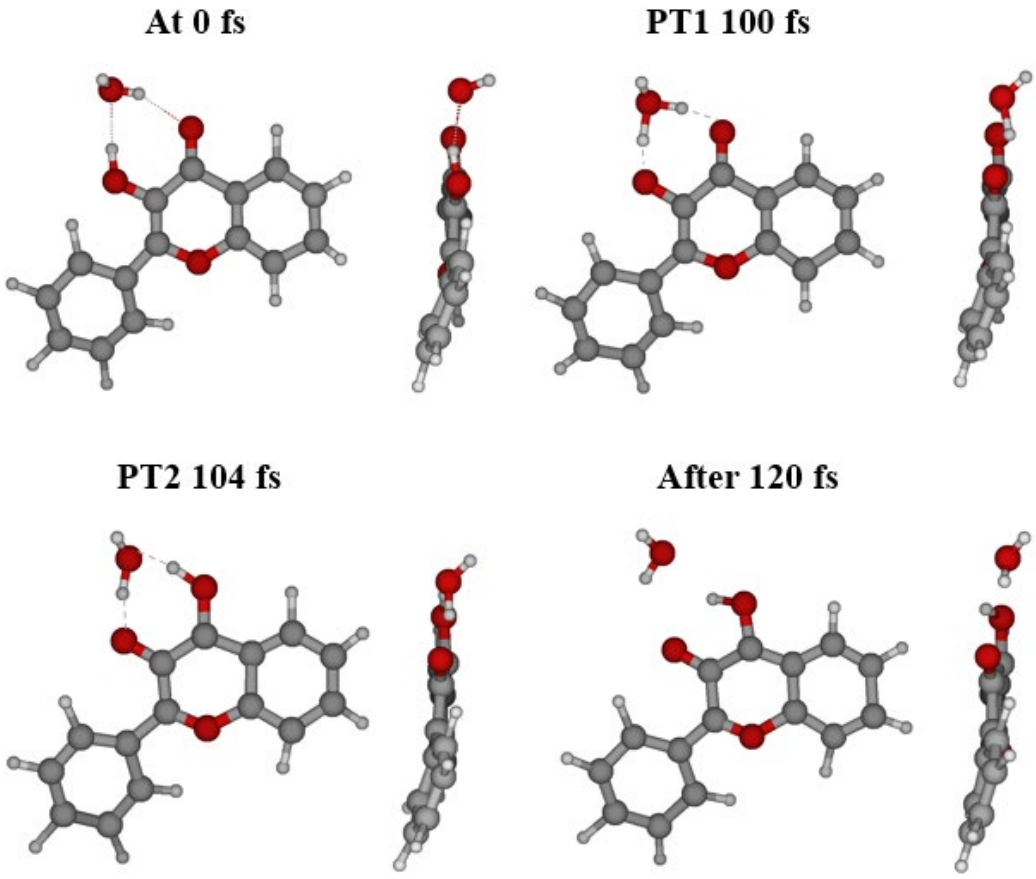

Figure 3.16 Snapshots of 3HF(H_2O) at different time along the ESInterPT dynamics simulations (left: front view, right: side view).

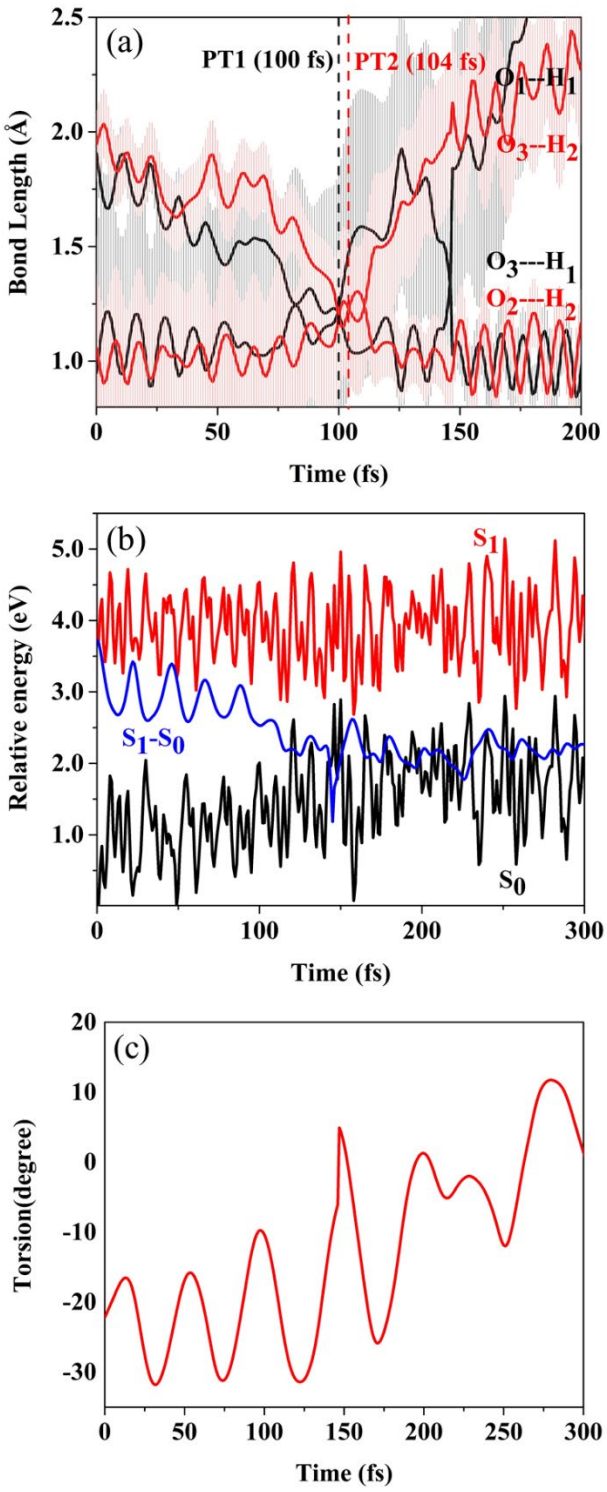

Figure 3.17 Average values over all active ESInterPT trajectories of 3HF(H_2O). (a) Time evolution of average breaking and forming bonds**.** The shaded areas are the standard deviation. (b) Average relative energies of excited state (S_1), ground state (S_0), and energy difference of S_1 and S_0 state (S_1-S_0). (c) Average torsion angle of 3HF(H_2O).